Science Advances
AAAS

advances.sciencemag.org/cgi/content/full/4/9/eaat7392/DC1

Supplementary Materials for

Programmable wettability on photocontrolled graphene film

Jie Wang, Wei Gao, Han Zhang, Minhan Zou, Yongping Chen*, Yuanjin Zhao*

*Corresponding author. Email: yjzhao@seu.edu.cn (Y.Z.); ypchen@mail.usts.edu.cn (Y.C.)

Published 14 September 2018, *Sci. Adv.* **4**, eaat7392 (2018)
DOI: 10.1126/sciadv.aat7392

The PDF file includes:

Other Supplementary Material for this manuscript includes the following:

(available at advances.sciencemag.org/cgi/content/full/4/9/eaat7392/DC1)

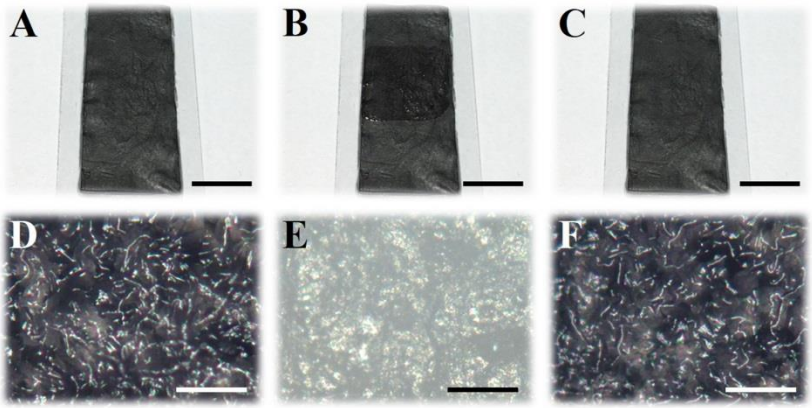

Fig. S1. Optical images of the PIPGF. (A-C) The optical images of the PIPGF before, under, and after irradiation, respectively. (D-F) The corresponding optical microscope images in (A-C). The scale bars are 1 cm in (A-C) and 100 μm in (D-F).

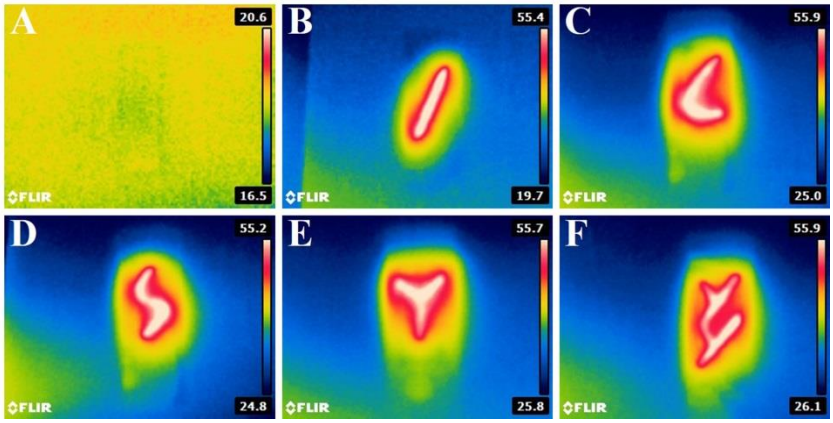

Fig. S2. Recorded temperature of the PIPGF with different pathways. (A) The temperature image of the PIPGF before turning on the laser. (B-F) Images showing the recorded temperature of the PIPGF with different droplet-guiding pathways. The highest spatial resolution of the patterned flow pathway here was around 1 mm. Approaches can be applied to for better resolution, such as adding lens in the front of the laser, decreasing the distance between the mask and the film as much as possible, and increasing the parallelism of the optical path.

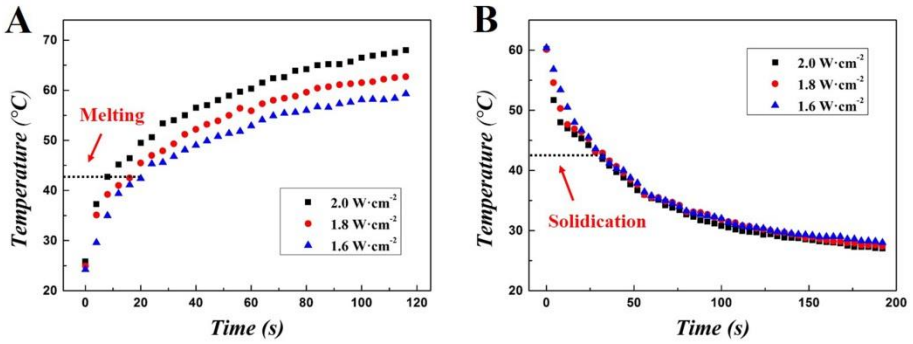

Fig. S3. Temperature change of the PIPGF during melting and solidification. The surface temperature change of the PIPGF monitored by an infrared camera with irradiation on (A) and off (B). 15 mg/mL GO was used to form the 300 μm thick film with 20 μL·cm^{-2} pure paraffin in this sample. The melting point and solidification point are around 42.5°C. With the correlation between the sample temperature and the time, the mass, the changed temperature, and the specific heat capacity of the sample, the time and power intensity of the irradiation, and the size of the irradiation area, the photo-thermal conversion efficiency of the PIPGF system under NIR irradiation can be achieved.

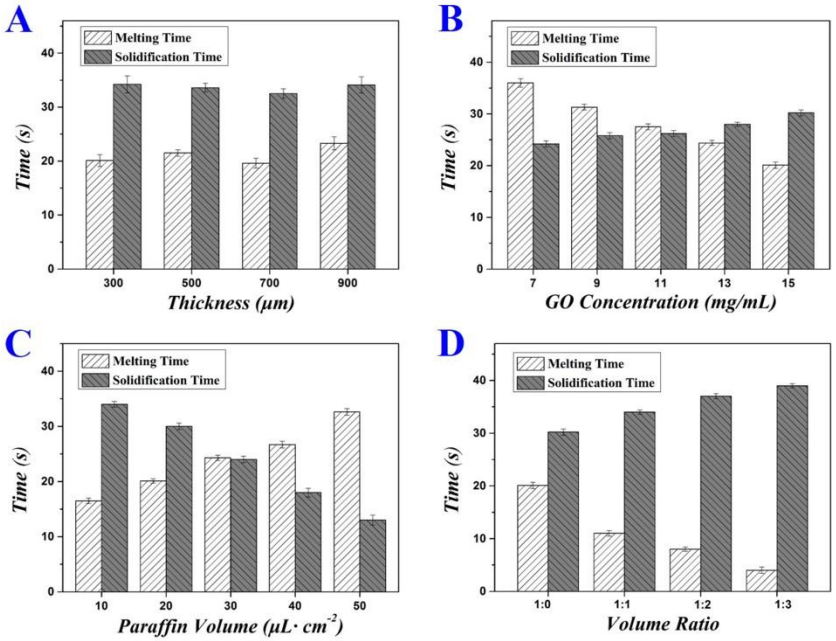

Fig. S4. Melting and solidification times of the PIPGF. The correlations of the melting time (from room temperature to the melting point) and solidification time (from 60°C to the solidification point) of the PIPGF and the sample thickness (A), the GO concentration (B), the paraffin volume (C), and the volume ratio of paraffin to liquid paraffin (D), respectively. 15 mg/mL GO was used to form the films with 20 μL·cm^{-2} pure paraffin in (A). GO was used to form the 300 μm thick film with 20 μL·cm^{-2} pure paraffin in (B). 15 mg/mL GO was used to form the 300 μm thick film with pure paraffin in (C). 15 mg/mL GO was used to form the 300 μm thick film with 20 μL·cm^{-2} mixed paraffin in (D).

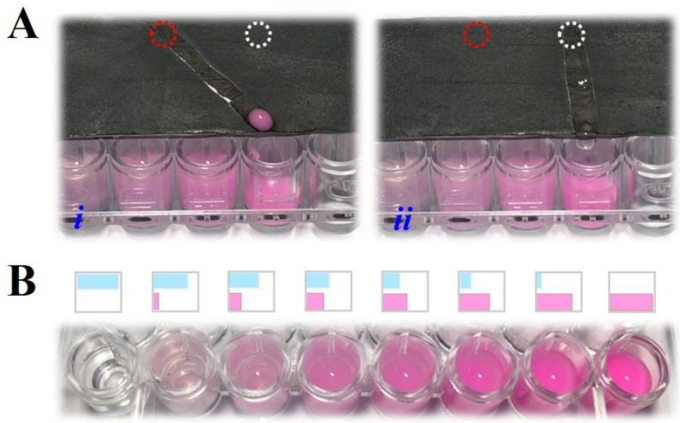

Fig. S5. Distributing different sample droplets. (A) The progress of distributing different sample droplets into the same well of the microplates. (B) Gradient concentrations of samples in the microplate wells were achieved by controlling the kinds and ratios of the sliding sample droplets.

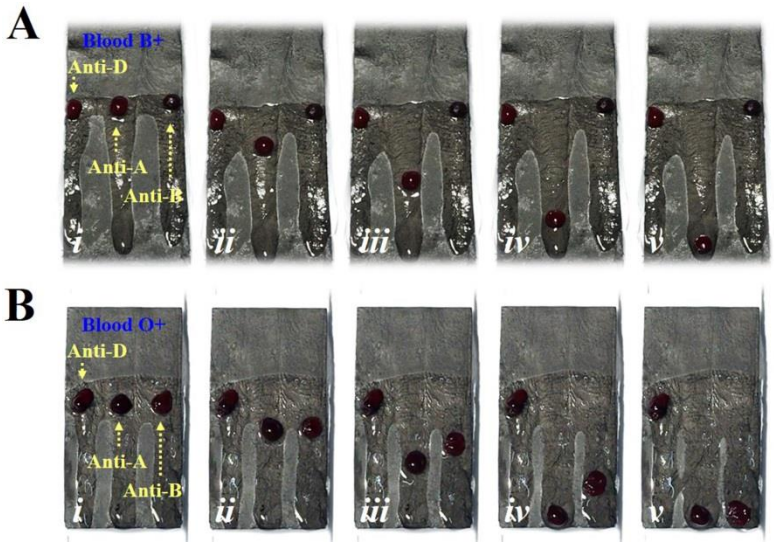

Fig. S6. PIPGF microreactor for grouping the blood samples B+ and O+. The progress of using the PIPGF microreactor for grouping the blood samples (A) B+ and (B) O+ by simply monitoring whether the composite blood droplets slid down or not. The antibodies are Anti-D, Anti-A, and Anti-B from left to right.

Table S1. Clotting times and sliding properties of the mixed blood droplets with different volume ratios of blood (A+) to antibody (anti-A). The clotting time had a positive correlation with the volume ratio and finally no obvious hemagglutination reaction could be observed for the lack of antibody. The excessively diluted RBCs precipitation droplet would slide down the surface when the ratio was less than 0.5. Thus, the ratio should be limited to the range of 0.5 to 3 and the second-level pathways should be switched on at least 4 s after mixing. 12 μL mixed blood droplets were tested on the PIPGF with the tilted angle of 20°.

Blood (A+) volume (μL)	Antibody (Anti-A) volume (μL)	Clotting time (s)	Sliding property
1	11	2	Sliding
2	10	2	Sliding
3	9	2	Sliding
4	8	2	Non-sliding
5	7	3	Non-sliding
6	6	3	Non-sliding
7	5	3	Non-sliding
8	4	3	Non-sliding
9	3	4	Non-sliding
10	2	No clear change	Sliding
11	1	No clear change	Sliding

Movie S1. Droplet mobility on a tilted PIPGF surface. The dynamic control process of droplet mobility on a tilted PIPGF surface (corresponding to **Fig. 3.**).

Movie S2. Programmed wettability pathways. The dynamic control of the droplet mobility on the PIPGF surface with different programmed wettability pathways (corresponding to **Fig. 4.**).

Movie S3. Manipulating droplet reactions and blood grouping. PIPGF with program wettability pathways as microfluidics for manipulating droplets reactions (corresponding to **Fig. 6A and 6B**) and the application of the PIPGF for blood grouping by monitoring whether the composite blood droplets slid down or not (corresponding to **Fig. 6C and 6D**).